

Comparative Studies of Dye Removal Efficiency of Surface Functionalized Nanoparticles with Other Adsorbents: Isotherm and Kinetic Study

ARTI JANGRA^{1,✉}, JAIVEER SINGH^{1,✉}, RADHIKA KHANNA^{2,✉}, PARVIN KUMAR^{1,✉}, SURESH KUMAR^{1,✉} and RAMESH KUMAR^{1,*✉}

¹Department of Chemistry, Kurukshetra University, Kurukshetra-136119, India

²Department of Chemistry, Babu Anant Ram Janta College, Kaul-136021, India

*Corresponding author: E-mail: rameshkumarkuk@gmail.com; rameshchemkuk@kuk.ac.in

Received: 10 August 2021;

Accepted: 23 September 2021;

Published online: 6 December 2021;

AJC-20595

In present work, the synthesis of the humic acid functionalized iron oxide nanoparticles and their application in water treatment are reported. The bare and humic acid functionalized iron oxide nanoparticles were characterized using different techniques such as X-ray diffraction (XRD), field emission scanning electron microscopy (FESEM), thermogravimetric analysis (TGA) and Fourier transform infrared (FTIR) spectroscopy. The synthesized magnetite nanoparticles coated with humic acid showed efficient removal of crystal violet dye from the aqueous solution. The functionalized magnetite nanoparticles were found to have higher adsorption capacity as compared to bare magnetite nanoparticles and the pure humic acid under specific conditions. The adsorption kinetics study was found in accordance with pseudo-second order kinetics while the isotherm data was observed to be in good agreement with the Tempkin isotherm. A comparative study of dye removal efficiency of humic acid functionalized magnetite nanoparticles with reported adsorbents has also been made.

Keywords: Adsorption studies, Crystal violet, Humic Acid, Magnetite nanoparticles.

INTRODUCTION

Organic substances such as organic dyes are released everyday in large quantities by the textile, paper and food industries which are responsible for the toxicity, colour, unpleasant odour and taste of the water resulting in deterioration of the quality of water. Further, this added toxicity has adverse effects on aquatic life. So, it becomes necessary to remove the coloured and toxic effluents from the water released from industries before it gets discharged into the rivers and other water bodies. Dyes are very dangerous to the health of living organism being both carcinogenic and toxic [1]. However, their removal from the industrial effluent is a challenging process.

Crystal violet dye, also known as hexamethyl pararosaniline chloride, is a triphenylmethane dye which is predominantly used in plethora of industries such as paper, fiber, leather, textile, paint, etc. It is a basic dye extensively employed as a microbiological stain, a dermatological agent [2] and in Gram's method of grouping bacteria. It is acutely noxious, which causes skin irritation and the gastrointestinal discomfort to the bodily cells. It is cationic dye, which is imperishable and carcinogenic in

nature and categorized as a defiant dye molecule owing to its high tenacity in the environment [3]. Higher amount of crystal violet dye residues present in water can diminish the level of oxygen in water streams and also influences the aquatic life and the photosynthesis process [4]. In human beings also, this dye may cause kidney and respiration problems along with eye irritation, which may lead to permanent blindness [5]. Consequently, water treatment containing crystal violet dye residues is essential for human being as well as environmental health. Many physical and chemical processes including adsorption [6], electrochemical oxidation [7], photocatalytic oxidation [8] and chemical oxidation [9] are being used for this purpose. However, among these processes, adsorption process is considered as more efficient method for the removal of dyes from the industrial effluents due to its low cost.

The use of activated carbon as the principal adsorbing agent has been reported to possess greater sorption capacity in dye confiscation due to its large surface area. But the activated carbon is barely used because of its higher cost. This demerit leads to the search of alternate adsorbents which are economic and environment friendly adsorbents e.g. biochar [10], coffee

husk [11], orange peel [12], *etc.* Several organic substances are also used for environmental remedy and are easily available. During the last few years, many researchers have evaluated the degradation of various cationic as well as anionic dyes such as crystal violet, methylene blue and indigo carmine [11], by using different adsorbents such as bottom ash [5], deoiled soya [5], chitosan [13], modified ash [14], reduced graphene oxide [15], acid treated kaolinite [16], sagaun sawdust [17], bentonite alginate composite [18], acid functionalized carboxymethyl cellulose materials [19], agricultural waste [20], acid based hydrogels [21], *etc.* from the aqueous solution.

However, the earlier reported adsorbing agents are being rarely used because of their low capacity to adsorb and difficulty to separate from aqueous solution. Therefore, the adsorbents which possess both properties *i.e.*, high adsorption capacity and ease of separation are receiving more attention. From last few years, nanosized magnetic particles have been extensively used in order to adsorb dye pollutants from the waste water because of their fascinating unique properties including large surface area to volume ratio, super paramagnetic character, their renewability as well as the ease of separation from the aqueous solution by applying external magnetic field. While bare magnetic iron oxide nanoparticles are oxidized and aggregated easily in the aqueous solutions that influences their adsorption capability. Therefore, several materials have been used to modify the surface of bare magnetic nanoparticles. For example, Yu *et al.* [22] used chitosan grafted on poly (quaternary ammonium)/Fe₃O₄ nanosized particles to remove food yellow 3 from synthetic solutions, whereas Massoudinejad *et al.* [23] studied the method of removing crystal violet dye using magnetic chitosan nanocomposite from aqueous solution. Muthukumaran *et al.* [24] investigated the isotherm and kinetic studies of crystal violet dye removal using surfactant modified magnetic nanoparticles. Elwakeel *et al.* [25] examined the cationic dye such as crystal violet adsorption from aqueous solutions by magnetic alginate beads. In this context, surface functionalized magnetite nanoparticles have been reported as an effective tool for the separation of toxic pollutants from the aqueous solution due to their better adsorption properties owing to their large surface area to volume ratio. At present, many organic as well as inorganic coating materials are being used to enhance the stability of nanoparticles and exploring their capability for the removal of contaminants from the aqueous solution [26-30]. Humic acid is an abundant natural organic macromolecule and highly reactive due to its unique amorphous structure. Various researches indicate that the humic acid has high affinity to bare Fe₃O₄ nanoparticles due to ligand exchange reactions between functional groups of humic acid and surface hydroxyl groups of magnetite nanoparticles. The coating of humic acid on bare Fe₃O₄ nanoparticles prevents the oxidation and further aggregation, which results in the improved stability of the coated nanoparticles. Humic acid and levulinic acid modified magnetic nanoparticles [31] have been reported for the exclusion of ciprofloxacin drug from the aqueous solution. Prompted by these views, the removal of crystal violet dye from the aqueous solution by humic acid coated magnetite nanoparticles is reported.

EXPERIMENTAL

Ferrous sulphate heptahydrate (FeSO₄·7H₂O, 98%), ferric chloride hexahydrate (FeCl₃·6H₂O, 97%), ammonium hydroxide solution (25%), crystal violet dye and humic acid were purchased from SRL (India) and used without any further purification.

Perkin-Elmer STA-6000 thermogravimetric analyzer was used for thermogravimetric analysis (temperature range 20-1000 °C). The size of bare and surface modified nanoparticles was determined with the help of field emission scanning electron microscope (Hitachi SU-8000). In addition, particle size analyzer (Microtrac W3602) was used to measure the average size of bare and coated magnetite nanoparticles. X-ray diffraction patterns were recorded on X-ray diffractometer retaining CuK α radiation ($\lambda = 1.540 \text{ \AA}$). UV spectra were obtained using a T90 PG Instrument Limited UV-visible spectrophotometer (900-190 nm). FTIR spectra were recorded on MB-3000 ABB spectrometer.

Synthesis of magnetic nanoparticles and their surface functionalization: The bare iron oxide nanoparticles were synthesized by adopting co-precipitation method followed by their surface functionalization with humic acid [32]. Briefly, 6.1 g of FeCl₃·6H₂O and 4.2 g FeSO₄·7H₂O were dissolved in 100 mL of deionized water. The resulting solution was heated gradually upto 90 °C followed by the rapid addition of 10 mL of ammonium hydroxide to it and black coloured bare iron oxide nanoparticles were precipitated. Then, 0.5 g of humic acid dissolved in 50 mL deionized water was added to these bare magnetite (Fe₃O₄) nanoparticles with continuous stirring for 0.5 h. The coated magnetic nanoparticles (HA@Fe₃O₄) were separated from the solution using decantation method by applying external magnetic field.

Preparation of stock solution of crystal violet dye: Stock solution of crystal violet (50 ppm) was prepared by dissolving 5 mg of crystal violet dye into 1 L of deionized water. Then, the stock solution was further diluted accordingly with deionized water to prepare solutions of various concentrations ranging from 10 pm to 50 ppm. The prepared stock solution and the solutions obtained after dilution were used to examine the effect of adsorption parameters such as effect of amount of adsorbent added and effect of contact time. Calibration curve for was obtained by plotting a graph between various concentrations of crystal violet dye and their absorbance at 590 nm to study the effects of above mentioned parameters.

Adsorption studies of HA@Fe₃O₄: The synthesized HA@Fe₃O₄ nanoparticles showed a remarkable removal efficiency of crystal violet dye from the aqueous solution by adsorption of dyes on their surface. Adsorption experiments were performed at room temperature using batch adsorption processes [33]. Adsorption behaviour was investigated for several parameters such as time of contact between the adsorbate (crystal violet dye) and adsorbent (HA@Fe₃O₄ nanoparticles); amount of adsorbent. The contact time was varied from 0 to 40 min and amount of adsorbent was varied from 5-25 mg, using 10 mL of adsorbate (20 mg/L). The equilibrium time was obtained using the fixed concentration of dye and adsorbent. Further,

the effect of variation in initial concentration of dye solution was also studied at equilibrium time keeping the amount of adsorbent fixed (5 mg). The adsorption capacity (q_e) was calculated by using eqn. 1:

$$q_e = \frac{(C_o - C_e)V}{m} \quad (1)$$

The percentage adsorption of the dye was determined using eqn. 2:

$$\text{Removal (\%)} = \frac{(C_o - C_e)}{C_o} \times 100 \quad (2)$$

The change in concentration of crystal violet dye after its adsorption from aqueous solution on to the surface of adsorbent (HA@Fe₃O₄ nanoparticles) was measured by recording absorbance at 590 nm.

RESULTS AND DISCUSSION

FTIR studies: FTIR spectrum of Fe₃O₄ nanoparticles exhibited peak near 600 cm⁻¹ which corresponds to Fe-O stretching vibration while another peak at 3300 cm⁻¹ may be assigned to O-H stretching. However, in the FTIR spectrum of HA@Fe₃O₄ nanoparticles, new peaks appeared at ~1638 and ~1416 cm⁻¹ may be assigned to asymmetric and symmetric stretching respectively, of carboxylate anion. These peaks were absent in IR spectrum of uncoated magnetite (Fe₃O₄) nanoparticles. So, the appearance of new peaks in the infrared spectrum of HA@Fe₃O₄ confirmed the coating of humic acid on the surface of Fe₃O₄ as these new peaks resemble the peaks present in the IR spectrum of pure humic acid [34]. The peaks in ~3500-3300 and ~1200 cm⁻¹ region present in infrared spectra of both pure humic acid and HA@Fe₃O₄ correspond to O-H group stretching and C-O stretching, respectively, present in humic acid and humic acid coated magnetite nanoparticles (Fig. 1).

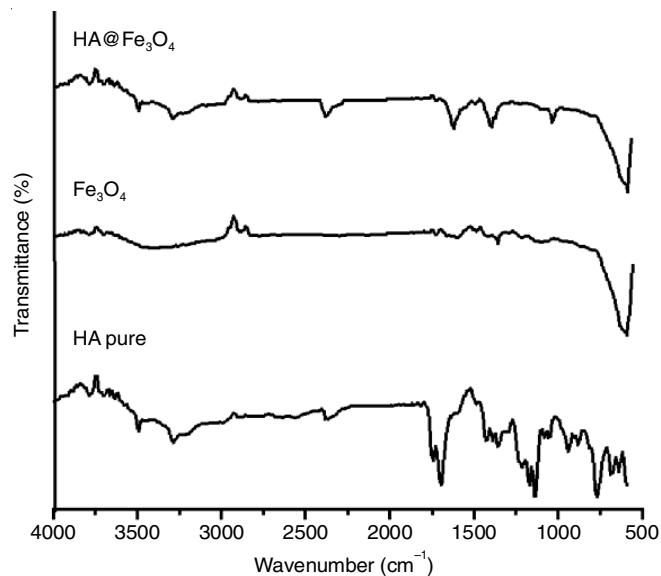


Fig. 1. FTIR spectra of neat Fe₃O₄ and HA@Fe₃O₄ nanoparticles

FESEM studies: The size of Fe₃O₄ nanoparticles and HA@Fe₃O₄ nanoparticles was determined using FESEM technique. The average size of Fe₃O₄ nanoparticles and HA@Fe₃O₄ nanoparticles was found to be 20 nm and 30 nm, respectively (Fig. 2). The increase in size of Fe₃O₄ magnetite nanoparticles after coating suggested the successful coating of humic acid on the surface of Fe₃O₄ magnetite nanoparticles.

XRD studies: XRD pattern of Fe₃O₄ and HA@Fe₃O₄ nanoparticles were recorded in 2θ range of 20-80° and the mean size of nanoparticles was theoretically calculated from XRD peaks, using the Debye-Scherrer equation ($d = 0.914\lambda/\beta \cos\theta$), where, λ is the wavelength (1.540 Å), β is full-width at half maximum and θ is Bragg angle in degree. The XRD pattern

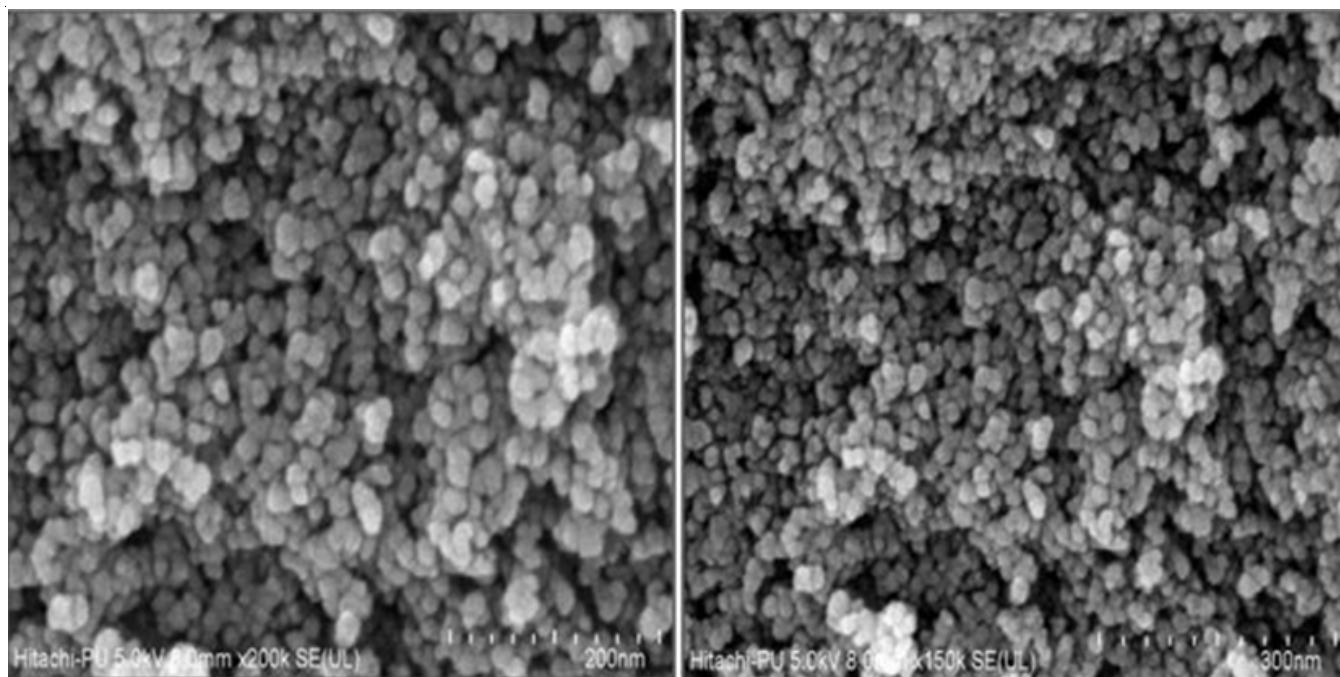


Fig. 2. FESEM image of neat Fe₃O₄ nanoparticles [1 division = 20 nm] and HA@Fe₃O₄ nanoparticles [1 division = 30 nm]

of Fe_3O_4 and $\text{HA}@\text{Fe}_3\text{O}_4$ nanoparticles showed sharp crystalline peaks, which clearly reveal their semi-crystalline nature (Fig. 3). The average diameter calculated for Fe_3O_4 and $\text{HA}@\text{Fe}_3\text{O}_4$ nanoparticles was found to be 17.8 nm and 26.4 nm, respectively. Interestingly, the size of Fe_3O_4 and $\text{HA}@\text{Fe}_3\text{O}_4$ nanoparticles calculated by Debye-Scherrer equation were found in close proximity with the size of these nanoparticles shown by FESEM technique (20 nm and 30 nm, respectively).

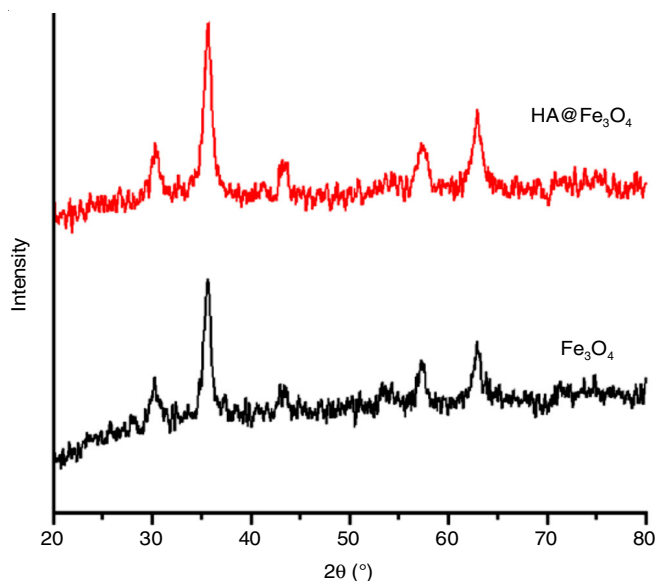


Fig. 3. XRD of neat Fe_3O_4 and $\text{HA}@\text{Fe}_3\text{O}_4$ nanoparticles

Thermogravimetric analysis: Thermogravimetric curves of $\text{HA}@\text{Fe}_3\text{O}_4$ nanoparticles showed different patterns from that of Fe_3O_4 nanoparticles. Thermogravimetric curve of Fe_3O_4 nanoparticles showed a fall in curve over a temperature range of 100–120 °C may be attributed to water loss from the sample. However, no change in TG curve was observed thereafter. But in case of $\text{HA}@\text{Fe}_3\text{O}_4$ nanoparticles, the TG curve showed the weight loss at ~100 °C due to moisture loss. In addition to this, significant weight loss was observed over a temperature range of 200 to 500 °C. This weight loss may be assigned to thermal decomposition of coating material *i.e.* humic acid (Fig. 4) present on the surface of $\text{HA}@\text{Fe}_3\text{O}_4$ nanoparticles and thus again confirming the coating of humic acid on surface of Fe_3O_4 nanoparticles.

Zeta potential: High magnitude of zeta potential reflects the more stability of nanoparticles which may be attributed due to electrostatic repulsion among the nanoparticles. The zeta potential for Fe_3O_4 and $\text{HA}@\text{Fe}_3\text{O}_4$ was found to be 22.4 mV and 35.9 mV, respectively indicated the more stability of $\text{HA}@\text{Fe}_3\text{O}_4$ nanoparticles as compared to Fe_3O_4 nanoparticles in the colloidal system. So, from zeta potential studies it can be inferred that the surface functionalization of Fe_3O_4 nanoparticles with humic acid enhanced their stability and prevented their aggregation also.

Magnetic properties of Fe_3O_4 and $\text{HA}@\text{Fe}_3\text{O}_4$ nanoparticles: Magnetic saturation (M_s) value of Fe_3O_4 nanoparticles was found to be 1.7545 emu/g whereas for $\text{HA}@\text{Fe}_3\text{O}_4$ nanoparticles, it was decreased to 1.2896 emu/g (Fig. 5). The decrease

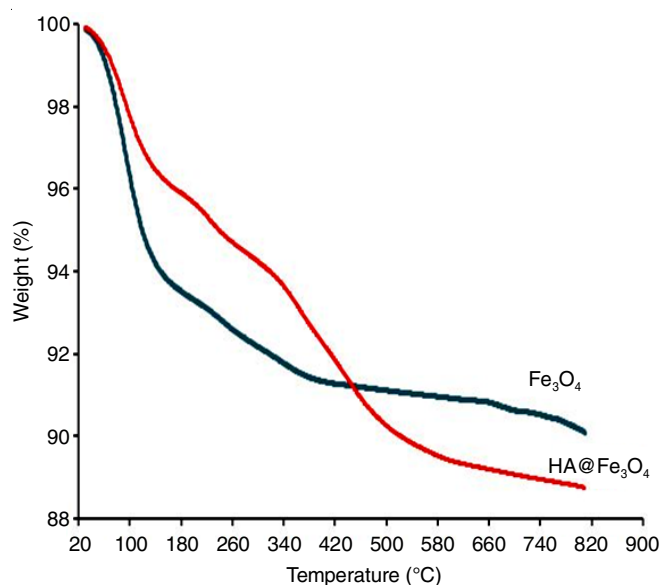


Fig. 4. TGA curves of neat Fe_3O_4 and $\text{HA}@\text{Fe}_3\text{O}_4$ nanoparticles

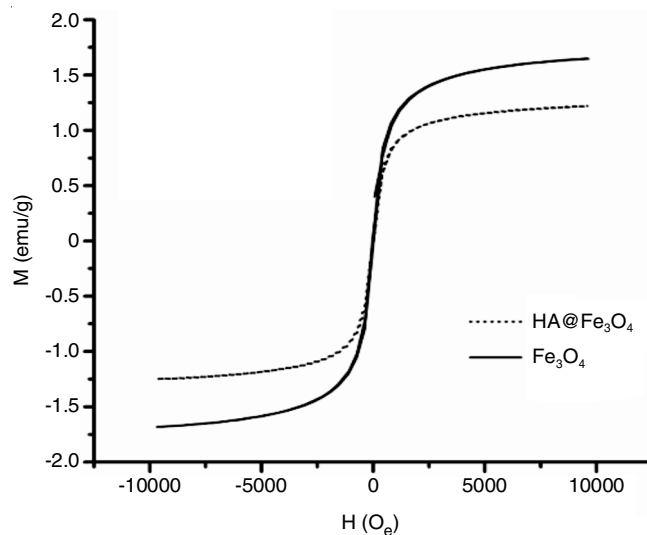


Fig. 5. VSM of neat Fe_3O_4 and $\text{HA}@\text{Fe}_3\text{O}_4$ nanoparticles

in M_s value of $\text{HA}@\text{Fe}_3\text{O}_4$ is quite obvious due to coating of non-magnetic material *i.e.* humic acid on the surface of magnetite Fe_3O_4 nanoparticles. However, from the M_s values, it is clear that magnetic properties of $\text{HA}@\text{Fe}_3\text{O}_4$ nanoparticles did not change significantly and thus their magnetic properties can be used for their separation from the solution by applying external magnetic field.

UV-VIS studies: UV spectrum of crystal violet dye solution was recorded before and after addition of $\text{HA}@\text{Fe}_3\text{O}_4$ nanoparticles to the crystal violet dye solution. The $\text{HA}@\text{Fe}_3\text{O}_4$ nanoparticles were removed from crystal violet dye solution after the completion of adsorption process by using external magnetic field. A significant decrease in the intensity of band in the UV spectrum of crystal violet dye solution was observed after the completion of adsorption process which revealed the removal of crystal violet dye from aqueous solution by $\text{HA}@\text{Fe}_3\text{O}_4$ nanoparticles. Furthermore, no additional peak corresponding to humic acid was observed in UV spectrum of

crystal violet dye solution after adsorption process that indicated the stability of humic acid coated over Fe_3O_4 magnetite nanoparticles in aqueous solution as no leaching of coating material occurred.

Effect on adsorption of crystal violet dye on the surface of $\text{HA}@Fe_3O_4$ nanoparticles with variation in different parameters

Effect of amount of $\text{HA}@Fe_3O_4$ nanoparticles and contact time: Batch adsorption trials were implemented to investigate the effects of various experimental adsorption parameters such as amount of $\text{HA}@Fe_3O_4$ nanoparticles, crystal violet dye concentration (varying from 5 mg/L to 20 mg/L) and contact time on the adsorption capacity of $\text{HA}@Fe_3O_4$.

Effect of amount of $\text{HA}@Fe_3O_4$ nanoparticles: The effect of variation in amount (ranging from 5 mg to 25 mg) of $\text{HA}@Fe_3O_4$ nanoparticles on the sorption of crystal violet dye, keeping its concentration fixed (20 mg/L) illustrated that the dye removal efficiency was increased with increase in amount of $\text{HA}@Fe_3O_4$ nanoparticles (Fig. 6). For instance, increase in amount of $\text{HA}@Fe_3O_4$ nanoparticles from 20 mg to 25 mg resulted in increase in percentage of adsorption of crystal violet dye from 84% to 96%.

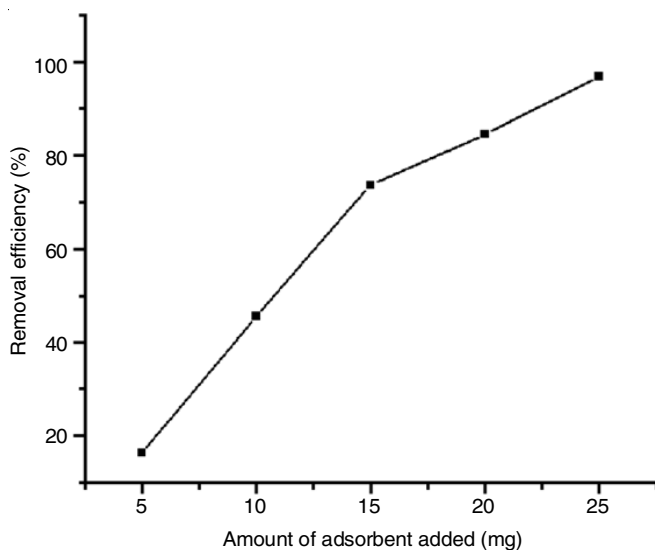


Fig. 6. Effect of amount of adsorbent added

Effect of contact time: Two models [35,36], the pseudo-first order kinetic model (eqn. 3) and the pseudo-second order kinetic model (eqn. 4) were employed to investigate the kinetics of dye sorption. The equilibrium point was attained after 0.5 h for HA-coated magnetic nanoparticles (Fig. 7).

$$\log(q_e - q_t) = \log q_e - \frac{k_1 t}{2.303} \quad (3)$$

$$\frac{t}{q_t} = \frac{1}{k_2 q_e^2} + \frac{t}{q_e} \quad (4)$$

where, q_e is the adsorption capacity at equilibrium while q_t represents the adsorption capacity at time t , k_1 and k_2 are the constants for pseudo-first order and pseudo-second order models, respectively.

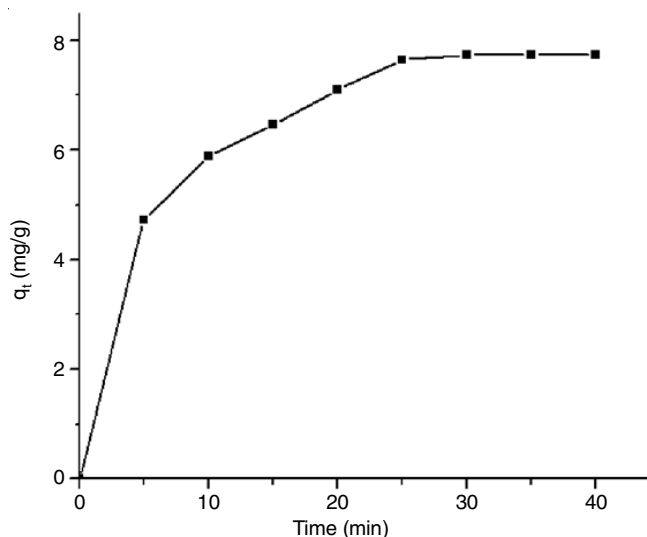


Fig. 7. Effect of Contact time

The correlation coefficient for pseudo-first order kinetic model was found comparatively low while correlation coefficient for pseudo second order was found to be 0.996, which implied that the adsorption process obeyed pseudo-second order kinetic model (Fig. 8).

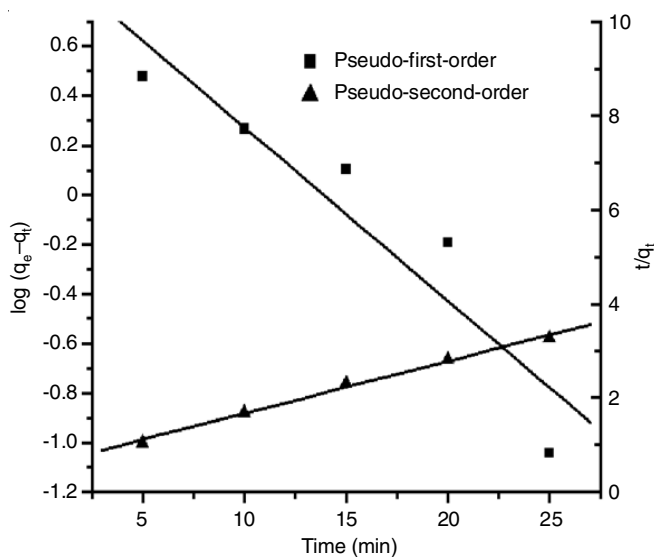


Fig. 8. Kinetic orders

Adsorption isotherm studies: The isotherm studies were accomplished to observe the interactions between crystal violet dye and $\text{HA}@Fe_3O_4$ nanoparticles. The adsorption capacities of $\text{HA}@Fe_3O_4$ nanoparticles were measured at fixed pH 8.3 and fixed concentration of $\text{HA}@Fe_3O_4$ nanoparticles (0.5 g/L) while varying the concentrations of crystal violet dye solution (5-20 mg/L). Several isotherm models were used to illustrate this study.

Langmuir isotherm: The Langmuir theory assumes a monolayer adsorption, which reveals that a single molecule can occupy a specific adsorption site [37]. The correlation coefficients and maximum adsorption loading capacity was calculated using Langmuir equation (eqn. 5).

$$q_e = \frac{q_m b C_e}{1 + b C_e} \quad (5)$$

where, q_e and q_m represents the equilibrium and maximum adsorption capacities, C_e denotes equilibrium concentrations. The correlation coefficient (R^2) was found to be 0.9025 whereas, the calculated value of maximum adsorption loading capacity was found to be 27.7 mg/g.

The favourability of the adsorption study under investigation was determined by using Langmuir isotherm (eqn. 6):

$$R_L = \frac{1}{1 + K_L C_0} \quad (6)$$

where, C_0 is the initial concentration. The calculated value of for the initial concentration of crystal violet was found to be 0.52, which lies in the range 0-1 suggesting that the adsorption process was a favourable process.

Freundlich isotherm: Freundlich theory assumes a heterogeneous adsorption, which implies that several adsorption energies are involved with different sites [38]. It shows the relationship between the amount adsorbed and the concentration at equilibrium. The correlation coefficient (R^2) and Freundlich isotherm constant, n was calculated using Freundlich isotherm equation (eqn. 7):

$$q_e = K_f \cdot C_e^{1/n} \quad (7)$$

The correlation coefficient (R^2) was found to be 0.9801 whereas, the value of n was found to be 1.29 indicating that the adsorption process was a physical process.

Tempkin isotherm: The Tempkin isotherm considered that the adsorption heat of all adsorbate molecules on the layer decreases in a linear manner due to the interactions between adsorbent and adsorbate [39]. Tempkin isotherm equation (eqn. 10) was used to calculate the correlation coefficient (R^2) and the Tempkin isotherm constants (A and B).

$$q_e = \frac{RT}{b} \ln AC_e \quad (8)$$

This can be linearized as follows:

$$q_e = \frac{RT}{b} \ln A + \frac{RT}{b} \ln C_e \quad (9)$$

$$q_e = b \ln A + b \ln C_e \quad (10)$$

where $B = RT/b$.

To study the Tempkin isotherm for dye adsorption onto adsorbent, a linear graph between q_e and $\ln C_e$ was plotted (Fig. 9). The value of A (0.599 L/g) indicated that the humic acid coated magnetite nanoparticles have significant potential for the adsorption of crystal violet whereas the value of B

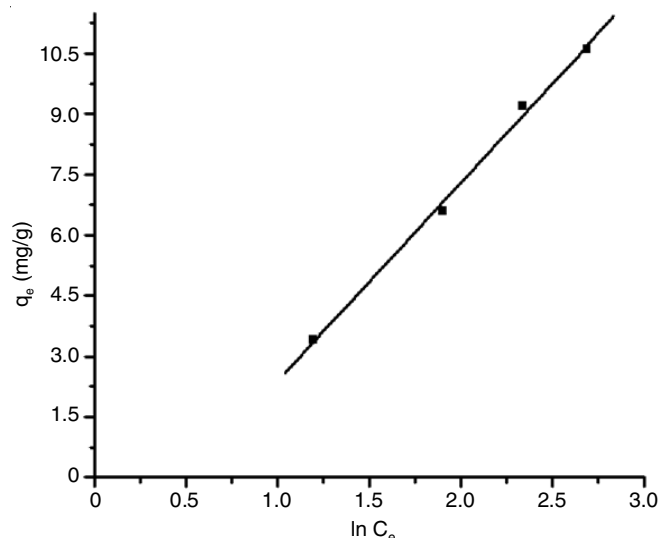


Fig. 9. Tempkin isotherm

(4.908 J/mol) revealed about the strong interactions between crystal violet dye and the humic acid coated magnetite nanoparticles. The constants and correlation coefficients (R^2) were obtained through linear fitting of curves (Table-1). By comparing the values of R^2 of all isotherm models, it was concluded that the adsorption isotherm could be well represented by Tempkin model of isotherm.

Comparative study of adsorption capacity of Fe₃O₄ nanoparticles, pure humic acid and HA@Fe₃O₄ nanoparticles: Iron oxide (Fe₃O₄) nanoparticles exhibited least sorption of crystal violet dye followed by pure humic acid. The removal of crystal violet dye from the aqueous solution was found maximum in case of HA@Fe₃O₄ nanoparticles. This suggested that Fe₃O₄ nanoparticles have no active sites required for the removal of crystal violet dye from the aqueous solution. However, powdered humic acid showed remarkable sorption of crystal violet dye over its surface, indicating that humic acid has active sites to adsorb crystal violet dye. This adsorption capacity of humic acid was increased significantly after it was coated on the surface of Fe₃O₄ nanoparticles (Fig. 10). This increase in adsorption capacity may be attributed to increased surface area to volume ratio of HA@Fe₃O₄ nanoparticles.

Comparative study of percentage crystal violet dye removal efficiency of HA@Fe₃O₄ nanoparticles with other reported adsorbents: The removal percentage efficiency of crystal violet dye of humic acid functionalized magnetite nanoparticles has been compared with crystal violet dye removal efficiency (%) shown by various reported adsorbents including bottom ash [5], de-oiled soya [5], acid functionalized biomass [40], modified ash [14], reduced graphene oxide [15], acid treated kaolinite [41], activated carbon from poultry litter [42],

TABLE-1
ISOTHERMS CONSTANTS

Langmuir		Freundlich		Tempkin		
R^2	q_m	R^2	n	R^2	A	B
0.9025	27.7 mg/g	0.9801	1.29	0.9960	0.599 L/g	4.908 J/mol

* q_m is maximum adsorption capacity, R is correlation coefficient, n is Freundlich constant, A and B are Tempkin constants.

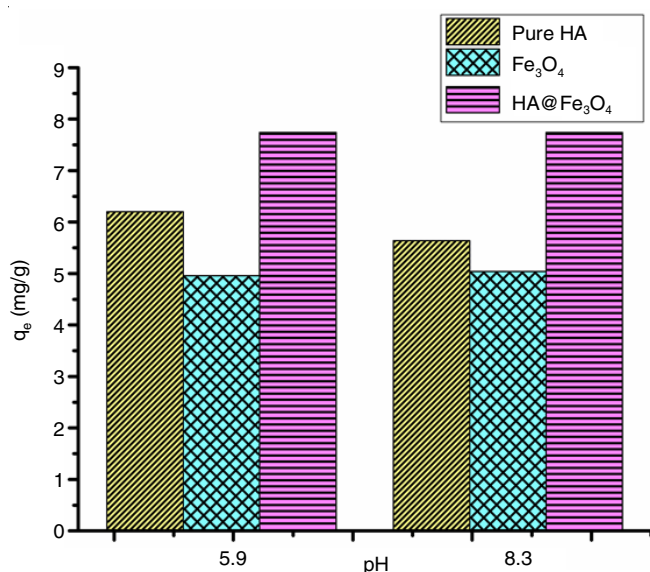


Fig. 10. Comparison graph of pure humic acid (HA) powder, Fe₃O₄ and HA@Fe₃O₄ nanoparticles for the adsorption of crystal violet dye

biowaste [43], acid based hydrogels [21], biochar [10], SPIONs [44], orange peel [12], magnetic orange peel [12], surfactant (SDS) modified magnetic nanoparticles [24] and magnetic chitosan nanocomposite [23] (Table-2). From this comparative study, it is clear that humic acid functionalized magnetite nanoparticles are more potential candidate as compared to above mentioned adsorbents for the removal of crystal violet residues from the aqueous solution.

TABLE-2
PERCENTAGE REMOVAL EFFICIENCY OF
VARIOUS ADSORBENTS FOR CRYSTAL VIOLET DYE

Adsorbent	Removal (%)
Bottom ash	95.00
De-oiled soya	78.00
Acid functionalized biomass	83.00
Modified ash	92.00
Reduced graphene oxide	95.00
Acid treated kaolinite	93.79
Activated carbon from poultry litter	92.03
Biowaste	85.00
Acid based hydrogels	95.00
Biochar	95.00
SPIONs	94.70
Orange peel and magnetic orange peel	86.00 & 91.10
Surfactant (SDS) modified magnetic nanoparticles	80.40
Magnetic chitosan nanocomposite	72.00
Humic acid functionalized magnetic nanoparticles (Present work)	96.00

Conclusion

Iron oxide (Fe₃O₄) nanoparticles and HA@Fe₃O₄ nanoparticles having a size of 20 and 30 nm respectively, were synthesized by using co-precipitation method. The vibrating sample magnetometer (VSM) studies revealed that the surface functionalization of Fe₃O₄ nanoparticles did not alter the magnetic properties of HA@Fe₃O₄ magnetic nanoparticles.

This is an important property of HA@Fe₃O₄ nanoparticles by virtue of which these can be easily separated from the solution under the influence of applied magnetic field. Moreover, HA@Fe₃O₄ nanoparticles exhibited remarkable adsorption capacity as these nanoparticles removed 96% of the crystal violet dye from the aqueous solution. This application of HA@Fe₃O₄ nanoparticles can be used in treatment of polluted water being released from dye industries. Moreover, the comparative study of crystal violet dye removal efficiency of humic acid functionalized magnetite nanoparticles with other adsorbents reached to the conclusion that the surface coated magnetite nanoparticles reported in present study have remarkable dye removal efficiency among all adsorbents. Hence, HA@Fe₃O₄ nanoparticles may be used on priority as an effective adsorbent to remove the crystal violet dye from the aqueous solution.

ACKNOWLEDGEMENTS

Two of the authors, Arti Jangra and Jaiveer Singh are highly thankful to UGC, New Delhi for providing the financial assistance in the form of Junior Research Fellowship.

CONFLICT OF INTEREST

The authors declare that there is no conflict of interests regarding the publication of this article.

REFERENCES

- P. Giridhar, A. Venugopalan and R. Parimalan, *J. Sci. Res. Rep.*, **3**, 327 (2014); <https://doi.org/10.9734/JSRR/2014/5870>
- G.K. Sarma, S. Sen Gupta and K.G. Bhattacharyya, *J. Environ. Manag.*, **171**, 1 (2016); <https://doi.org/10.1016/j.jenvman.2016.01.038>
- T. Su, L. Wu, X. Pan, C. Zhang, M. Shi, R. Gao, X. Qi and W. Dong, *J. Colloid Interface Sci.*, **542**, 253 (2019); <https://doi.org/10.1016/j.jcis.2019.02.025>
- H. Mittal, A.A. Alili, P.P. Morajkar and S.M. Alhassan, *J. Mol. Liq.*, **323**, 115034 (2021); <https://doi.org/10.1016/j.molliq.2020.115034>
- A. Mittal, J. Mittal, A. Malviya, D. Kaur and V.K. Gupta, *J. Colloid Interface Sci.*, **343**, 463 (2010); <https://doi.org/10.1016/j.jcis.2009.11.060>
- F. Ferrero, *J. Environ. Sci.*, **22**, 467 (2010); [https://doi.org/10.1016/S1001-0742\(09\)60131-5](https://doi.org/10.1016/S1001-0742(09)60131-5)
- K. Zhao, G. Zhao, P. Li, J. Gao, B. Lv and D. Li, *Chemosphere*, **80**, 410 (2010); <https://doi.org/10.1016/j.chemosphere.2010.04.019>
- R. Jain, M. Mathur, S. Sikarwar and A. Mittal, *J. Environ. Manage.*, **85**, 956 (2007); <https://doi.org/10.1016/j.jenvman.2006.11.002>
- S.H. Chang, K.S. Wang, H.C. Li, M.Y. Wey and J.D. Chou, *J. Hazard. Mater.*, **172**, 1131 (2009); <https://doi.org/10.1016/j.jhazmat.2009.07.106>
- M.A. Zazycki, P.A. Borba, R.N.F. Silva, E.C. Peres, D. Perondi, G.C. Collazzo and G.L. Dotto, *Adv. Powder Technol.*, **30**, 1494 (2019); <https://doi.org/10.1016/j.apt.2019.04.026>
- G.K. Cheruiyot, W.C. Wanyonyi, J.J. Kiplimo and E.N. Maina, *Sci. African*, **5**, e00116 (2019); <https://doi.org/10.1016/j.sciaf.2019.e00116>
- M. Ahmed, F. Mashkoor and A. Nasar, *Groundwater Sustain. Dev.*, **10**, 100322 (2020); <https://doi.org/10.1016/j.gsd.2019.100322>
- L. Zhou, J. Jin, Z. Liu, X. Liang and C. Shang, *J. Hazard. Mater.*, **185**, 1045 (2011); <https://doi.org/10.1016/j.jhazmat.2010.10.012>

14. M. Harja, G. Ciobanu, L. Favier, L. Bulgariu and L. Rusu, *Bul. Inst. Polit. Iasi*, **66**, 28 (2016).
15. M.H. Kahsay, N. Belachew, A. Tadesse and K. Basavaiah, *RSC Adv.*, **10**, 34916 (2020); <https://doi.org/10.1039/D0RA07061K>
16. G.K. Sarma, S. Sen Gupta and K.G. Bhattacharyya, *SN Appl. Sci.*, **1**, 211 (2019); <https://doi.org/10.1007/s42452-019-0216-y>
17. S.D. Khattri and M.K. Singh, *Environ. Prog. Sustain. Energy*, **31**, 435 (2012); <https://doi.org/10.1002/ep.10567>
18. R. Fabryanty, C. Valencia, F.E. Soetaredjo, J.N. Putro, S.P. Santoso, A. Kurniawan, Y.H. Ju and S. Ismadi, *J. Environ. Chem. Eng.*, **5**, 5677 (2017); <https://doi.org/10.1016/j.jece.2017.10.057>
19. A.M. Omer, G.S. Elgarhy, G.M. El-Subruiti, R.E. Khalifa and A.S. Eltaweil, *Int. J. Biol. Macromol.*, **148**, 1072 (2020); <https://doi.org/10.1016/j.ijbiomac.2020.01.182>
20. N. Khoshnamvand, S. Ahmadi and F. Kord Mostafapour, *J. Appl. Pharm. Sci.*, **7**, 79 (2017).
21. P. Ilgin, H. Ozay and O. Ozay, *React. Funct. Polym.*, **142**, 189 (2019); <https://doi.org/10.1016/j.reactfunctpolym.2019.06.018>
22. C. Yu, J. Geng, Y. Zhuang, J. Zhao, L. Chu, X. Luo, Y. Zhao and Y. Guo, *Carbohydr. Polym.*, **152**, 327 (2016); <https://doi.org/10.1016/j.carbpol.2016.06.114>
23. M. Massoudinejad, H. Rasoulzadeh and M. Ghaderpoori, *Carbohydr. Polym.*, **206**, 844 (2019); <https://doi.org/10.1016/j.carbpol.2018.11.048>
24. C. Muthukumar, V.M. Sivakumar and M. Thirumarimurugan, *J. Taiwan Inst. Chem. Eng.*, **63**, 354 (2016); <https://doi.org/10.1016/j.jtice.2016.03.034>
25. K.Z. Elwakeel, A.A. El-Bindary, A.Z. El-Sonbati and A.R. Hawas, *Can. J. Chem.*, **95**, 807 (2017); <https://doi.org/10.1139/cjc-2016-0641>
26. B.S Inbaraj and B.H. Chen, *Bioresour. Technol.*, **102**, 8868 (2011); <https://doi.org/10.1016/j.biortech.2011.06.079>
27. D.H.K. Reddy and S.M. Lee, *Adv. Colloid Interface Sci.*, **201-202**, 68 (2013); <https://doi.org/10.1016/j.cis.2013.10.002>
28. A. Adak, M. Bandyopadhyay and A. Pal, *Sep. Purif. Technol.*, **44**, 139 (2005); <https://doi.org/10.1016/j.seppur.2005.01.002>
29. J. Hu, G. Chen and I.M.C. Lo, *Water Res.*, **39**, 4528 (2005); <https://doi.org/10.1016/j.watres.2005.05.051>
30. J. Hu, I. Lo and G. Chen, *Sep. Purif. Technol.*, **56**, 249 (2007); <https://doi.org/10.1016/j.seppur.2007.02.009>
31. S.T. Danalioglu, S.S. Bayazit, Ö. Kerkez, B.G. Alhogbi and M. Abdel Salam, *Chem. Eng. Res. Des.*, **123**, 259 (2017); <https://doi.org/10.1016/j.cherd.2017.05.018>
32. J. Liu, Z. Zhao and G. Jiang, *Environ. Sci. Technol.*, **42**, 6949 (2008); <https://doi.org/10.1021/es800924c>
33. A. Mohammadi, H. Daemi and M. Barikani, *Int. J. Biol. Macromol.*, **69**, 447 (2014); <https://doi.org/10.1016/j.ijbiomac.2014.05.042>
34. H. Niu, D. Zhang, S. Zhang, X. Zhang, Z. Meng and Y. Cai, *J. Hazard. Mater.*, **190**, 559 (2011); <https://doi.org/10.1016/j.jhazmat.2011.03.086>
35. S. Lagergren, *Vetenskademien Handl.*, **24**, 1 (1898).
36. Y.S. Ho and G. McKay, *Process Biochem.*, **34**, 451 (1999); [https://doi.org/10.1016/S0032-9592\(98\)00112-5](https://doi.org/10.1016/S0032-9592(98)00112-5)
37. I. Langmuir, *J. Am. Chem. Soc.*, **40**, 1361 (1918); <https://doi.org/10.1021/ja02242a004>
38. H.M.Z. Freundlich, *Phys. Chem.*, **57**, 385 (1906).
39. M.J. Tempkin and V. Pyzhev, *Wuli Huaxue Xuebao*, **12**, 217 (1940).
40. A.H. Jawad, A.S. Abdulhameed and M.S. Mastuli, *J. Taibah Univ. Sci.*, **14**, 305 (2020); <https://doi.org/10.1080/16583655.2020.1736767>
41. O. Sakin Omer, M.A. Hussein, B.H.M. Hussein and A. Mgaidi, *Arab. J. Chem.*, **11**, 615 (2018); <https://doi.org/10.1016/j.arabjc.2017.10.007>
42. A.S. Yusuff, O.A. Ajayi and L.T. Popoola, *Sci. African*, **13**, e00850 (2021); <https://doi.org/10.1016/j.sciaf.2021.e00850>
43. M. Akram, M. Salman, R. Rehman, U. Farooq, S. Tahir and H. Nazir, *J. Chem.*, **2021**, 1 (2021); <https://doi.org/10.1155/2021/5549536>
44. S.M. Abobakr, N.I. Abdo and R.A. Mansour, *J. Environ. Stud.*, **6**, 1 (2020); <https://doi.org/10.13188/2471-4879.1000028>